

DESY/06-236, MS-TP-06-34  
 RM3-TH/07-1, ROM2F/2007/02  
 SFB/PPP-06-57

# Dynamical Twisted Mass Fermions with Light Quarks



**Ph. Boucaud<sup>(a)</sup>, P. Dimopoulos<sup>(b)</sup>, F. Farchioni<sup>(c)</sup>, R. Frezzotti<sup>(b)</sup>,  
 V. Gimenez<sup>(d)</sup>, G. Herdoiza<sup>(b)</sup>, K. Jansen<sup>(e)</sup>, V. Lubicz<sup>(f)</sup>,  
 G. Martinelli<sup>(g)</sup>, C. McNeile<sup>(h)</sup>, C. Michael<sup>(h)</sup>, I. Montvay<sup>(i)</sup>,  
 D. Palao<sup>(d)</sup>, M. Papinutto<sup>(f)</sup>, J. Pickavance<sup>(h)</sup>, G.C. Rossi<sup>(b)</sup>,  
 L. Scorzato<sup>(j)</sup>, A. Shindler<sup>(e)</sup>, S. Simula<sup>(f)</sup>, C. Urbach<sup>(h)</sup>, U. Wenger<sup>(k)</sup>**

<sup>(a)</sup> Laboratoire de Physique Théorique (Bât. 210), Université de Paris XI,  
 Centre d'Orsay, 91405 Orsay-Cedex, France

<sup>(b)</sup> Dip. di Fisica, Università di Roma Tor Vergata and INFN, Sez. di Roma Tor Vergata,  
 Via della Ricerca Scientifica, I-00133 Roma, Italy

<sup>(c)</sup> Universität Münster, Institut für Theoretische Physik,  
 Wilhelm-Klemm-Strasse 9, D-48149 Münster, Germany

<sup>(d)</sup> Dep. de Física Teòrica and IFIC, Univ. de València,  
 Dr.Moliner 50, E-46100 Burjassot, Spain

<sup>(e)</sup> NIC, DESY, Zeuthen, Platanenallee 6, D-15738 Zeuthen, Germany

<sup>(f)</sup> Dip. di Fisica, Università di Roma Tre and INFN, Sez. di Roma III,  
 Via della Vasca Navale 84, I-00146 Roma, Italy

<sup>(g)</sup> Dip. di Fisica, Università di Roma "La Sapienza", and INFN, Sezione di Roma,  
 P.le A. Moro 2, I-00185 Rome, Italy

<sup>(h)</sup> Theoretical Physics Division, Dept. of Mathematical Sciences,  
 University of Liverpool, Liverpool L69 7ZL, UK

<sup>(i)</sup> Deutsches Elektronen-Synchrotron DESY, Notkestr. 85, D-22607 Hamburg, Germany

<sup>(j)</sup> ECT\* Strada delle Tabarelle 286, I-38050 Villazzano (TN), Italy

<sup>(k)</sup> Institute for Theoretical Physics, ETH Zürich, CH-8093 Zürich, Switzerland

## Abstract

We present results of dynamical simulations of  $N_f = 2$  degenerate Wilson twisted mass quarks at maximal twist in the range of pseudo scalar masses  $300 \text{ MeV} \lesssim m_{\text{PS}} \lesssim 550 \text{ MeV}$ . Reaching such small masses was made possible owing to a recently developed variant of the HMC algorithm. The simulations are performed at one value of the lattice spacing  $a \lesssim 0.1 \text{ fm}$ . In order to have  $\mathcal{O}(a)$  improvement and aiming at small residual  $\mathcal{O}(a^2)$  cutoff effects, the theory is tuned to maximal twist by requiring the vanishing of the untwisted quark mass. Precise results for the pseudo scalar decay constant and the pseudo scalar mass are confronted with chiral perturbation theory predictions and the low energy constants  $F$ ,  $\bar{l}_3$  and  $\bar{l}_4$  are evaluated with small statistical errors.

## 1 Introduction

The Wilson twisted mass formulation of lattice QCD, though a rather recent approach, has been by now well established. It amounts to adding a twisted mass term to the standard, un-improved Wilson-Dirac operator [1] leading to so-called Wilson twisted mass fermions [2, 3].

Besides being a theoretically sound formulation of lattice QCD, Wilson twisted mass fermions offer a number of advantages when tuned to maximal twist: (i) in this case automatic  $\mathcal{O}(a)$  improvement is obtained by tuning only one parameter, the bare untwisted quark mass, while avoiding additional tuning of operator-specific improvement-coefficients; (ii) the mixing pattern in the renormalisation process can be significantly simplified; (iii) the twisted mass provides an infra-red regulator helping to overcome possible problems with ergodicity in molecular dynamics based algorithms<sup>1</sup>.

In the *quenched approximation*, these expectations – based on general field theoretical and chiral perturbation theory ( $\chi$ PT) related arguments [2, 3, 11, 12, 13, 14, 15] – could be verified in actual simulations [16, 17, 18, 19]:  $\mathcal{O}(a)$  improvement is indeed realised when the theory is tuned to maximal twist. Moreover, it has been shown that a particular realisation of maximal twist, requiring parity restoration, also suppresses the  $\mathcal{O}(a^2)$  cut-off effects substantially, even at small quark masses corresponding to values of the pseudo scalar mass of  $m_{\text{PS}} \lesssim 300 \text{ MeV}$ . In addition, with the twisted mass parameter as an infra-red cut-off in place, substantially smaller quark masses could be obtained, compared to those reachable by standard or  $\mathcal{O}(a)$  improved Wilson fermions which are plagued by so-called exceptional configuration problems in the quenched approximation. In Refs. [20, 21, 22] it was shown that “wrong chirality” mixing effects

---

<sup>1</sup>Although in the light of recent algorithmic developments [4, 5, 6, 7, 8, 9] this property does not seem to be that important anymore, we consider it still to be an advantage to have an infra-red regulator in the theory which helps in stabilising the simulations. For a recent stability analysis of pure Wilson fermion simulations see Ref. [10]

in the renormalisation process are substantially reduced. In Ref. [11] it was proved that all such mixings can be eliminated if a mixed action with maximally twisted sea quarks and appropriately chosen Osterwalder–Seiler valence fermions is employed. For a further discussion of the potential of twisted mass QCD on the lattice, see Refs. [23, 24, 25, 26].

The main drawback of the twisted mass approach is the explicit breaking of parity and isospin symmetry which are only restored when the continuum limit is reached. However, due to  $\mathcal{O}(a)$  improvement, this breaking is an  $\mathcal{O}(a^2)$  effect as confirmed by simulations performed in the quenched approximation [27, 28]. For recent reviews of the status of Wilson twisted mass fermions see Refs. [29, 30, 31] and references therein.

It is the main goal of our collaboration to compute a number of phenomenologically relevant quantities with *dynamical quarks, in the continuum limit* and at *small values of the pseudo scalar mass*. As a first step in this direction we here present results for  $N_f = 2$  mass-degenerate quarks at a fixed lattice spacing  $a \lesssim 0.1$  fm. We have so far concentrated on the pseudo scalar mass  $m_{\text{PS}}$ , covering a range of values  $300\text{MeV} \lesssim m_{\text{PS}} \lesssim 550\text{MeV}$ , the pseudo scalar decay constant  $f_{\text{PS}}$  and the static inter-quark force parameter  $r_0$  at five values of the quark mass. A wider range of physical observables will be addressed in the future. The results for  $m_{\text{PS}}$  and  $f_{\text{PS}}$  are confronted with predictions of  $\chi\text{PT}$  which allows extracting the low-energy constants  $\bar{l}_3$ ,  $\bar{l}_4$ ,  $F$  and  $B_0$  of the corresponding effective chiral Lagrangian. We also provide a determination of the size of isospin violation measured from the mass splitting between the lightest charged and neutral pseudo scalar particles. First accounts of our work were presented at recent conferences, see Refs. [32, 33]. In this publication we will focus on the results of our present simulations obtained at one value of  $\beta$  and one volume. We shall provide, in a forthcoming paper [34], a comprehensive description of our analysis procedure and address systematic errors by including future runs on larger lattices, at different values of  $\beta$  and with extended statistics. Related works with Wilson fermions at similar small pseudo scalar meson masses are published in Refs. [35, 36, 37].

## 2 Choice of Lattice Action

The Wilson twisted mass fermionic lattice action for two flavours of degenerate quarks reads (in the so called twisted basis [2] and fermion fields with continuum dimensions)

$$\begin{aligned}
 S_{\text{tm}} = a^4 \sum_x \left\{ \bar{\chi}_x \left[ m_0 + i\gamma_5 \tau_3 \mu + \frac{4r}{a} \right] \chi_x \right. \\
 \left. + \frac{1}{2a} \sum_{\nu=1}^4 \bar{\chi}_x \left[ U_{x,\nu}(-r + \gamma_\nu) \chi_{x+\hat{\nu}} + U_{x-\hat{\nu},\nu}^\dagger(-r - \gamma_\nu) \chi_{x-\hat{\nu}} \right] \right\}, \tag{1}
 \end{aligned}$$

where  $am_0$  is the bare untwisted quark mass and  $a\mu$  the bare twisted mass,  $\tau_3$  is the third Pauli matrix acting in flavour space and  $r$  is the Wilson parameter, which we set to one in our simulations. Twisted mass fermions are said to be at *maximal twist* if the bare untwisted mass is tuned to its critical value,  $m_{\text{crit}}$ . We will discuss later how this can be achieved in practice.

In the gauge sector we use the so called tree-level Symanzik improved gauge action (tlSym) [38], which includes besides the plaquette term  $U_{x,\mu,\nu}^{1\times 1}$  also rectangular  $(1 \times 2)$  Wilson loops  $U_{x,\mu,\nu}^{1\times 2}$

$$S_g = \frac{\beta}{3} \sum_x \left( b_0 \sum_{\substack{\mu,\nu=1 \\ 1 \leq \mu < \nu}}^4 \{1 - \text{Re Tr}(U_{x,\mu,\nu}^{1\times 1})\} + b_1 \sum_{\substack{\mu,\nu=1 \\ \mu \neq \nu}}^4 \{1 - \text{Re Tr}(U_{x,\mu,\nu}^{1\times 2})\} \right) \quad (2)$$

with  $\beta$  the bare inverse coupling,  $b_1 = -1/12$  and the (proper) normalisation condition  $b_0 = 1 - 8b_1$ . Note that at  $b_1 = 0$  this action becomes the usual Wilson plaquette gauge action.

## 2.1 $\mathcal{O}(a)$ improvement

As mentioned before,  $\mathcal{O}(a)$  improvement can be obtained by tuning Wilson twisted mass fermions to maximal twist. In fact, it was first proved in Ref. [3] that parity even correlators are free from  $\mathcal{O}(a)$  lattice artifacts at maximal twist by using spurionic symmetries of the lattice action. Later on it was realised [12, 31] that a simpler proof is possible based on the parity symmetry of the continuum QCD action and the use of the Symanzik effective theory.

From this latter way of proving  $\mathcal{O}(a)$  improvement, it becomes also clear how to define maximal twist: first, choose an operator odd under parity (in the physical basis) which has a zero expectation value in the continuum. Second, at a non-vanishing value of the lattice spacing tune the expectation value of this operator to zero by adjusting the value of  $am_0$ . This procedure, which has been proposed in [39, 40] and has been theoretically analysed in [12], is sufficient to define maximal twist independently of the chosen operator. To approach smoothly the continuum limit this tuning has to be performed at fixed physical situation while decreasing the lattice spacing.

It was shown in an extended scaling test in the quenched approximation, that  $\mathcal{O}(a)$  improvement works extremely well for maximally twisted mass quarks [16, 17, 18]. In the context of this scaling test, the method of setting the so-called PCAC mass to zero was found to be very successful, in agreement with theoretical considerations [15, 13, 12]. Here the PCAC mass

$$m_{\text{PCAC}} = \frac{\sum_{\mathbf{x}} \langle \partial_0 A_0^a(x) P^a(0) \rangle}{2 \sum_{\mathbf{x}} \langle P^a(x) P^a(0) \rangle}, \quad a = 1, 2 \quad (3)$$

is evaluated at large enough time separation, such that the pion ground state is dominant. To see that the procedure of defining  $am_{\text{crit}}$  from the vanishing of

$m_{\text{PCAC}}$  is the appropriate one, it is enough to recall that under that condition the multilocal operator  $\sum_{\mathbf{x}} A_0^a(x) P^a(0)$  becomes, in the physical basis, the parity odd operator  $\epsilon^{3ab} \sum_{\mathbf{x}} \bar{\psi} \gamma_0 \tau^b \psi(x) \bar{\psi} \gamma_5 \tau^a \psi(0)$ .

In principle one could think of determining  $am_{\text{crit}}$  at each value of  $a\mu$  at which simulations are performed, possibly followed by an extrapolation to vanishing  $a\mu$ . The strategy we are following in this paper is, instead, to take the value of  $am_{\text{crit}}$  from the simulation at the lowest available value  $a\mu_{\text{min}} \ll a\Lambda_{\text{QCD}}$ . In this situation  $\mathcal{O}(a)$  improvement is still guaranteed, because working at  $\mu_{\text{min}}$  merely leads to  $\mathcal{O}(a\mu_{\text{min}}\Lambda_{\text{QCD}})$  effects in  $m_{\text{crit}}$  and  $\mathcal{O}(a^2\mu_{\text{min}}\Lambda_{\text{QCD}})$  relative corrections in physical quantities [12].

## 2.2 Phase Structure

In order to understand our choice of the gauge action, it is important to realise that Wilson-type fermions have a non-trivial phase structure at finite lattice spacing: in a series of publications [41, 39, 40, 29, 42, 43] the phase structure of lattice QCD was explored. For lattice spacings  $a \geq 0.15$  fm clear signals of first order phase transitions at the chiral point were found. The strength of those phase transitions weakens when the continuum limit is approached. This phase transition was identified to be a *generic* property of Wilson-type fermions since the phenomenon takes place for the pure Wilson as well as the Wilson twisted mass formulation [2, 3] of lattice QCD. Also the properties of physical quantities measured in both metastable branches of this first order phase transition were studied and compared to results of  $\chi$ PT [13, 15, 44, 45, 46, 47] finding that (lattice)  $\chi$ PT describes the simulation data quite well. This is somewhat surprising since the simulation data were obtained at rather coarse values of the lattice spacing and at rather heavy pseudo scalar masses, where the applicability of  $\chi$ PT may be questionable.

A very important consequence of the first order phase transition phenomenon is that at non-vanishing lattice spacing, simulations cannot be performed with pseudo scalar mesons below a certain minimal mass value. From lattice  $\chi$ PT analyses it is expected that this minimal value of the pseudo scalar mass goes to zero with a rate of  $\mathcal{O}(a)$ . In different words, given a value of the pseudo scalar mass,  $m_{\text{PS}}$ , one can always find a value of the lattice spacing  $a_{\text{max}}(m_{\text{PS}})$ , such that simulations at  $a < a_{\text{max}}(m_{\text{PS}})$  can be safely performed. For example, when the Wilson plaquette gauge action is used one finds  $a_{\text{max}} \approx 0.07$  fm to realise a pseudo scalar mass of about 300MeV [43].

The phase structure of lattice QCD with Wilson-type fermions has previously been addressed: there have been investigations concerning the Aoki-phase [48] in Refs. [49, 50] at large gauge couplings corresponding to values of the lattice spacing  $a \geq 0.2$  fm. In other studies [51, 52, 53] signals of first order phase transitions were found for Wilson fermions with and without the clover term, see also Ref. [54]. In Ref. [55] a speculative picture of the phase structure of Wilson

$\beta$	$L^3 \cdot T$	$a\mu_{\min}$	$\kappa_{\text{crit}}(a\mu_{\min})$	$r_0/a$
3.9	$24^3 \cdot 48$	0.004	0.160856	5.22(2)

**Table 1:** Simulation parameters. We denote by  $a\mu_{\min}$  the smallest value of the twisted mass parameter  $a\mu$  at which we have performed simulations. At this value of  $a\mu$  we determined the critical mass  $m_{\text{crit}}$ , or, equivalently the critical hopping parameter  $\kappa_{\text{crit}} = 1/(8 + 2am_{\text{crit}})$ . The value of  $r_0/a$  has been extrapolated to the physical point, where  $m_{\text{PS}} = 139.6$  MeV.

lattice QCD has been given and in Ref. [56] an analysis within the framework of  $\chi$ PT has been reported. A detailed understanding of the generic phase structure was obtained in the 2-dimensional Gross-Neveu model, see Refs. [57, 58, 59]. Of course, it is unclear how much these last results are applicable to 4-dimensional lattice QCD.

In order to choose a gauge action for our production simulations we studied the phase structure employing a number of different gauge actions: the standard Wilson plaquette gauge action [1] ( $b_1 = 0$  in Eq. (2)), the DBW2 gauge action [60] ( $b_1 = -1.4088$ ) and the tree-level Symanzik improved gauge action [38] ( $b_1 = -1/12$ ). A marked dependence of the strength of the phase transition on the choice of the gauge action has been found. In particular, these investigations revealed that the DBW2 and the tlSym gauge actions substantially weaken the effect of the first order phase transition and in particular the value of  $a_{\text{max}}$  increases when the coefficient  $b_1$  in Eq. (2) is moved away from zero [40, 43]. We refer to Refs. [29, 31] for summaries of these results.

The DBW2 gauge action appears to lead to a bad scaling behaviour [61, 62, 63] and a slow convergence of perturbation theory [64], whereas the tlSym gauge action is expected to show – by construction – a good scaling behaviour and a fast convergence of perturbation theory. Therefore, the tlSym gauge action looks like a good compromise between the Wilson gauge action which is most strongly affected by the first order phase transition and the DBW2 gauge action.

## 3 Numerical Results

### 3.1 Set-up

In this letter we will present results at a fixed value of the lattice spacing of  $a \lesssim 0.1$  fm only. In table 1 we provide the value of  $a\mu_{\min}$  at which we imposed the vanishing of  $m_{\text{PCAC}}$  (Eq. (3)) and thus determined  $am_{\text{crit}}$ . In table 2 we list the values of the quark mass  $am_{\text{PCAC}}$ , the pseudo scalar mass  $am_{\text{PS}}$ , the pseudo scalar decay constant  $af_{\text{PS}}$ ,  $r_0/a$  and the plaquette integrated autocorrelation time at all values of the twisted mass parameter  $a\mu$ . All other parameters were kept fixed as specified in table 1.

The algorithm we used is a HMC algorithm with mass preconditioning [4, 65]

$a\mu$	$am_{\text{PS}}$	$af_{\text{PS}}$	$am_{\text{PCAC}}$	$r_0/a$	$\tau_{\text{int}}(P)$
0.0040	0.13587(68)	0.06531(40)	-0.00001(27)	5.196(28)	55(17)
0.0064	0.16937(36)	0.07051(35)	-0.00009(17)	5.216(27)	23(07)
0.0085	0.19403(50)	0.07420(24)	-0.00052(17)	5.130(28)	13(03)
0.0100	0.21004(52)	0.07591(40)	-0.00097(26)	5.143(25)	15(04)
0.0150	0.25864(70)	0.08307(34)	-0.00145(42)	5.038(24)	06(02)

**Table 2:** Results from simulations at  $\beta = 3.9$  using the simulation parameters listed in table 1. The measurements were started after 1500 equilibration trajectories and are based on 5000 equilibrated trajectories.

and multiple time scale integration described in detail in Ref. [8]. The trajectory length  $\tau$  was set to  $\tau = 1/2$  in all our runs. Our estimates of the plaquette integrated autocorrelation time  $\tau_{\text{int}}(P)$  quoted in table 2 are in units of  $\tau = 1/2$ . Note that our estimates of the autocorrelation times of quantities such as  $am_{\text{PS}}$  or  $af_{\text{PS}}$  are found to be substantially smaller, typically by a factor of 5-10, than those reported in the table for the plaquette.

As discussed above, maximal twist is realised in our simulations by tuning  $m_0$  to obtain a vanishing PCAC quark mass  $am_{\text{PCAC}}$  at the smallest value  $a\mu_{\text{min}}$  of the twisted mass parameter  $a\mu$ . From table 2 one can see that this condition has been numerically realised with good accuracy, which in this context means  $m_{\text{PCAC}}(\mu_{\text{min}})/\mu_{\text{min}} < a\Lambda_{\text{QCD}}$  within statistical errors ( $a\Lambda_{\text{QCD}} \sim 0.1$  in our case). Once this is achieved, the (weak)  $\mu$ -dependence of  $m_{\text{PCAC}}$ , which is visible in fig. 1(a), is an  $\mathcal{O}(a)$  cutoff effect that merely modifies the  $\mathcal{O}(a^2)$  artifacts in physical observables, as already mentioned in section 2.1.

In order to make maximum use of the gauge configurations, we evaluate connected meson correlators using a stochastic method to include all spatial sources. The method involves a stochastic source (Z(2)-noise in both real and imaginary part) for all colour and spatial indices at one Euclidean time slice. By solving for the propagator from this source for each of the 4 spin components, we can construct zero-momentum meson correlators from any bilinear at the source and sink. Four inversions of the Dirac matrix per Euclidean time slice value are necessary, since we chose to use only one stochastic sample per gauge configuration. This “one-end” method is similar to that pioneered in Ref. [66] and implemented in Ref. [67]. We also employ a fuzzed source [68] of the extent of 6 lattice spacings to enable studying non-local meson creation and destruction operators. This allowed us to obtain very stable effective masses and to confirm the extraction of the pion ground state.

In general, we save a gauge configuration every second trajectory and analyse meson correlators as described above from a selection of different Euclidean time slice sources. To reduce autocorrelations, we only use the same time slice source every 8-10 trajectories. Our primary statistical error was obtained with the so



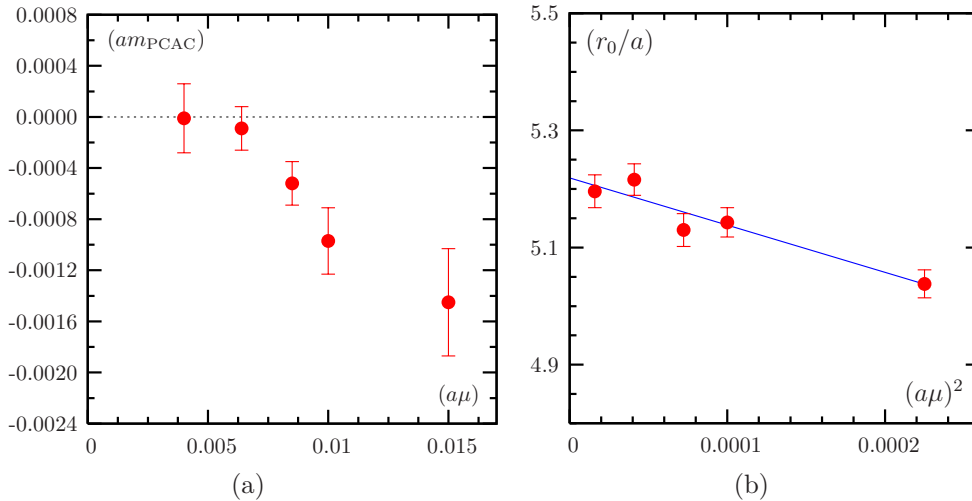


**Figure 1:** (a) PCAC quark mass  $am_{\text{PCAC}}$  as function of  $a\mu$  and (b) Sommer parameter  $(r_0/a)$  as functions of  $(a\mu)^2$ . The solid line in subfigure (b) represents a linear fit in  $(a\mu)^2$  to the data.

called  $\Gamma$ -method as described in Ref. [69] and cross-checked with a bootstrap analysis and a jack-knife analysis of blocked data. For a detailed description of our error analysis we refer to a forthcoming paper of our collaboration [34].

### 3.2 Force parameter $r_0$

In simulations of the quenched approximation of lattice QCD, the Sommer parameter  $r_0$  [70] with a value of 0.5 fm, was widely used to set the lattice scale. While  $(r_0/a)$  is measurable to good accuracy in lattice QCD simulations it has the drawback that its value in physical units is not known very well. Therefore, it becomes necessary to determine the scale using other quantities which are experimentally accessible with high precision, such as  $m_\pi$ ,  $f_\pi$ ,  $m_K$ ,  $f_K$  or  $m_{K^*}$ . In fact, in this paper we attempt to determine the lattice scale by fitting  $\chi$ PT based formulae to our precise data for  $f_{\text{PS}}$  and  $m_{\text{PS}}$ , using the physical values for  $m_\pi$  and  $f_\pi$  as inputs. From this analysis, we obtain a value of the lattice spacing which is 10% lower than the value obtained by setting  $r_0 = 0.5$  fm.

Our results for  $(r_0/a)$  are reported in table 2 and plotted in figure 1(b). Within the current errors the mass dependence of this quantity appears to be weak. Since  $r_0$  is a pure gauge quantity, it should be a function of  $(a\mu)^2$  and indeed, a linear fit in  $(a\mu)^2$  describes the data rather well as shown in figure 1(b). From the fit we obtain a value for  $r_0/a = 5.22(2)$  at the physical point, where  $a\mu = a\mu_\pi$  (see below), as also quoted in table 1.



### 3.3 $f_{\text{PS}}$ and $m_{\text{PS}}$ as a function of the quark mass

The *charged* pseudo scalar meson mass  $am_{\text{PS}}$  is as usual extracted from the time exponential decay of appropriate correlation functions <sup>2</sup>. In contrast to pure Wilson fermions, for maximally twisted mass fermions an exact lattice Ward identity allows to extract the (charged) pseudo scalar meson decay constant  $f_{\text{PS}}$  from the relation

$$f_{\text{PS}} = \frac{2\mu}{m_{\text{PS}}^2} |\langle 0|P^1(0)|\pi\rangle|, \quad (4)$$

with no need to compute any renormalisation constant since  $Z_P = 1/Z_\mu$  [2]. We give our results for  $m_{\text{PS}}$  and  $f_{\text{PS}}$  in table 2.

We now discuss whether the continuum  $\chi$ PT formulae can reproduce the data in table 2 for  $am_{\text{PS}}$  and  $af_{\text{PS}}$ . In our  $\chi$ PT based analysis, we take into account finite size corrections because on our lattices at the lowest and next-to-lowest  $\mu$ -values they turn out to affect  $am_{\text{PS}}$  and, in particular,  $af_{\text{PS}}$  in a significant way. We have used continuum  $\chi$ PT to describe consistently the dependence of the data both on the finite spatial size ( $L$ ) and on  $\mu$ .

We fit the appropriate ( $N_f = 2$ )  $\chi$ PT formulae [71, 72]

$$m_{\text{PS}}^2(L) = 2B_0\mu \left[ 1 + \frac{1}{2}\xi\tilde{g}_1(\lambda) \right]^2 [1 + \xi \log(2B_0\mu/\Lambda_3^2)], \quad (5)$$

$$f_{\text{PS}}(L) = F [1 - 2\xi\tilde{g}_1(\lambda)] [1 - 2\xi \log(2B_0\mu/\Lambda_4^2)], \quad (6)$$

to our raw data for  $m_{\text{PS}}$  and  $f_{\text{PS}}$  simultaneously. Here

$$\xi = 2B_0\mu/(4\pi F)^2, \quad \lambda = \sqrt{2B_0\mu L^2}. \quad (7)$$

The finite size correction function  $\tilde{g}_1(\lambda)$  was first computed by Gasser and Leutwyler in Ref. [71] and is also discussed in Ref. [72] from which we take our notation (except that our normalisation of  $f_\pi$  is 130.7 MeV). In Eqs. (5) and (6) NNLO  $\chi$ PT corrections are assumed to be negligible. The formulae above depend on four unknown parameters,  $B_0$ ,  $F$ ,  $\Lambda_3$  and  $\Lambda_4$ , which will be determined by the fit.

We determine  $a\mu_\pi$ , the value of  $a\mu$  at which the pion assumes its physical mass, by requiring that the ratio  $[\sqrt{m_{\text{PS}}^2(L=\infty)}]/f_{\text{PS}}(L=\infty)$  takes the value  $(139.6/130.7) = 1.068$ . From the knowledge of  $a\mu_\pi$  we can evaluate  $\bar{l}_{3,4} \equiv \log(\Lambda_{3,4}^2/m_\pi^2)$  and using  $f_\pi$  the value of the lattice spacing  $a$  in fm.

In order to estimate the statistical errors affecting our fit values we generate at each of the  $\mu$ -values 1000 bootstrap samples for  $m_{\text{PS}}$  and  $f_{\text{PS}}$  extracted from the bare correlators, blocked with block-size of 32. For each sample (combining all masses) we then fit  $m_{\text{PS}}^2$  and  $f_{\text{PS}}$  simultaneously as a function of  $\mu$ . From the 1000 fits we obtain 1000 bootstrap samples for  $2aB_0$ ,  $aF$ ,  $\log(a^2\Lambda_{3,4}^2)$ ,  $a\mu_\pi$ ,  $a$

---

<sup>2</sup>Concerning results on the neutral pion mass,  $am_{\text{PS}}^0$ , see section (3.4).

and  $\bar{l}_{3,4}$ , respectively, from which we compute the corresponding error estimates, taking in this way the statistical correlation between  $f_{\text{PS}}$  and  $m_{\text{PS}}$  into account.

For our lightest four  $\mu$ -values, we find an excellent fit to our data on  $f_{\text{PS}}$  and  $m_{\text{PS}}$  (see figures 2 and 3). The fitted values of the four parameters are

$$\begin{aligned} 2aB_0 &= 4.99(6), \\ aF &= 0.0534(6), \\ \log(a^2\Lambda_3^2) &= -1.93(10), \\ \log(a^2\Lambda_4^2) &= -1.06(4). \end{aligned} \tag{8}$$

Our data are clearly sensitive to  $\Lambda_3$  as visualised in figure 2(a). We obtain

$$a\mu_\pi = 0.00078(2), \quad \bar{l}_3 = 3.65(12), \quad \bar{l}_4 = 4.52(06) \tag{9}$$

which compares nicely with other determinations (for a review see Ref. [73]). Including also our results from  $a\mu = 0.0150$  in the fit gives an acceptable description of  $m_{\text{PS}}^2$  but misses the data for  $f_{\text{PS}}$ , as shown in figures 2(b) and 3. Note, however, that in Eqs. (5, 6), and thus in the fit results (8, 9), a number of systematic errors as discussed below are not included.

The values presented here should hence be taken as a first estimate, the validity of which will be checked in the future. Nevertheless, the statistical accuracy we are able to achieve implies that there is a very good prospect of obtaining accurate and reliable values for the low-energy constants from Wilson twisted mass fermion simulations.

Since we have obtained an excellent description of our pseudo scalar mesons, we can use our fit to extract the lattice spacing. Based on the physical value of  $f_\pi$ , we get

$$a = 0.087(1) \text{ fm}. \tag{10}$$

Using the value of  $r_0/a$  reported in table 1, this lattice calibration method yields  $r_0 = 0.454(7) \text{ fm}$ .

We now discuss the possible sources of systematic error. Our analysis is based on lattice determinations of properties of pseudo scalar mesons with masses in the range 300 to 500 MeV on lattices with a spatial size slightly above 2 fm. Systematic errors can arise from several sources:

(i) Finite lattice spacing effects. Preliminary results at a smaller value of the lattice spacing that were presented in Refs. [32, 33] suggest that  $\mathcal{O}(a)$  improvement is nicely at work and that residual  $\mathcal{O}(a^2)$  effects are small.

(ii) Finite size effects. In order to check that next to leading order (continuum)  $\chi\text{PT}$  adequately describes these, we are presently performing a run at  $\beta = 3.9$  and  $a\mu = 0.004$  on a  $32^3 \cdot 64$  lattice.

(iii) Mass difference of charged and neutral pseudo scalar meson. In the appropriate lattice  $\chi\text{PT}$  power-counting for our values of the lattice spacing and quark masses, i.e.  $a \sim \mu \sim p^2$ , one gets the order of magnitude relation

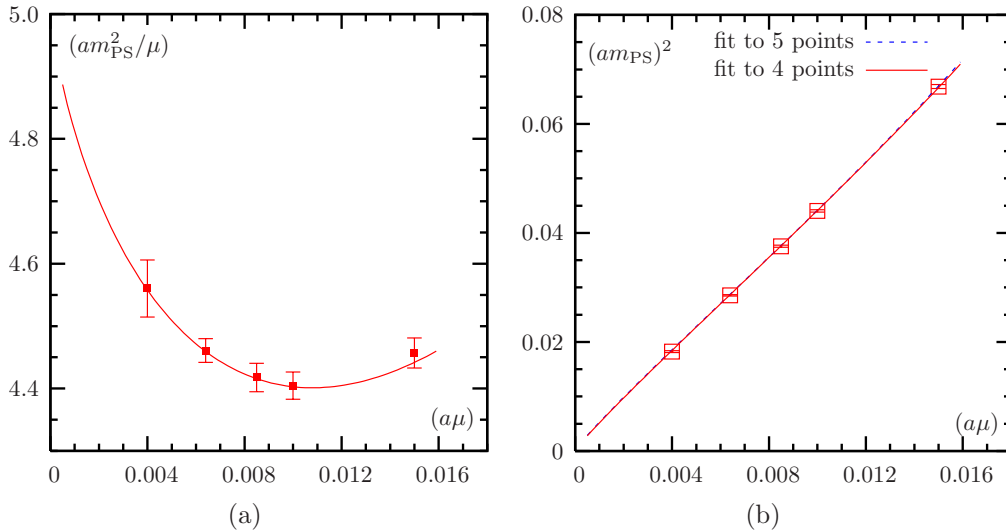


**Figure 2:** In (a) we show  $(am_{PS})^2/(a\mu)$  as a function of  $a\mu$ . In addition we plot the  $\chi$ PT fit with Eq. (5) to the data from the lowest four  $\mu$ -values. In (b) we show  $(am_{PS})^2$  as a function of  $a\mu$ . Here we present two  $\chi$ PT fits with Eq. (5), one taking all data points and one leaving out the point at the largest value  $a\mu = 0.015$ . In both figures (a) and (b) we show finite size corrected ( $L \rightarrow \infty$ ) data points.

$(m_{PS})^2 - (m_{PS}^0)^2 = \mathcal{O}(a^2\Lambda_{\text{QCD}}^4) = \mathcal{O}(p^4)$ , from which it follows that to the order we have been working the effects of the pion mass splitting do not affect, in particular, the finite size correction factors for  $m_{PS}$  and  $f_{PS}$ . In spite of these formal remarks, it is possible, however, that the fact that the neutral pion is lighter than the charged one (by about 20% at  $a\mu = 0.0040$ , see section (3.4)) makes inadequate the continuum  $\chi$ PT description of finite size effects adopted in the present analysis. This caveat represents a further motivation for simulations on larger lattices, which will eventually resolve the issue.

(iv) Extrapolation to physical quark masses. We are assuming that  $\chi$ PT at next to leading order for the  $N_f = 2$  case is appropriate to describe the quark mass dependence of  $m_{PS}^2$  and  $f_{PS}$  up to  $\sim 450$ – $500$  MeV. Our lattice data are consistent with this, but it would be useful to include higher order terms in the  $\chi$ PT fits as well as more values of  $a\mu$  to check this assumption. The effect of strange quarks in the sea should also be explored.

### 3.4 Effects of Isospin Breaking

In this section we report the results of some quantitative investigation of the effects of isospin breaking in the twisted mass formulation of lattice QCD at finite lattice spacing. This effect is expected to be largest in the mass splitting between the lightest charged and uncharged pseudo scalar mesons. A first analysis at  $a\mu = 0.004$ , taking the disconnected contribution in the neutral channel fully

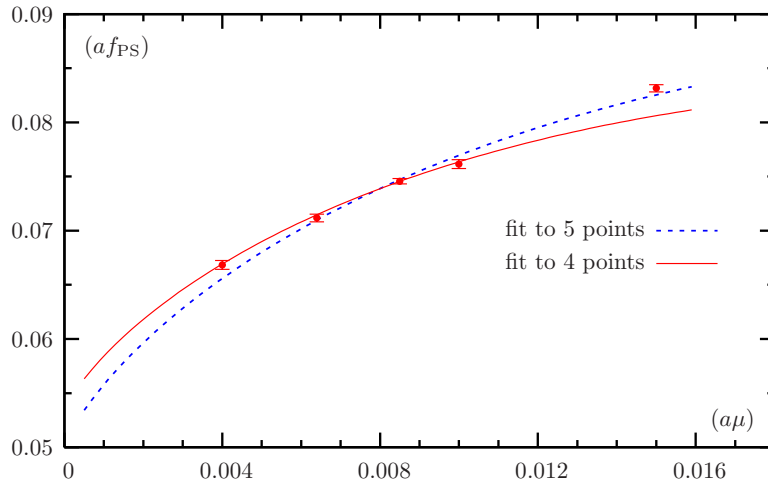


**Figure 3:** We show  $af_{\text{PS}}$  as a function of  $a\mu$  together with fits to  $\chi$ PT formula Eq. (6). We present two fits, one taking all data and one leaving out the point at the largest value  $a\mu = 0.015$ . We show finite size corrected ( $L \rightarrow \infty$ ) data points.

into account, shows that the uncharged pseudo scalar meson is about 20% lighter than the charged one. We obtain

$$am_{\text{PS}}^{\pm} = 0.1359(7), \quad am_{\text{PS}}^0 = 0.111(11),$$

or, expressed differently,  $r_0^2((m_{\text{PS}}^0)^2 - (m_{\text{PS}}^{\pm})^2) = c(a/r_0)^2$  with  $c = -4.5(1.8)$ . This coefficient is a factor of 2 smaller than the value found in quenched investigations [28]. Note that the uncharged pion being lighter than the charged one is compatible with predictions from lattice  $\chi$ PT if the first order phase transition scenario is realised [45, 47, 44]. For an investigation of isospin breaking effects in  $\chi$ PT see also Ref. [74].

The disconnected correlations needed for the  $\pi^0$  meson are evaluated using a stochastic (Gaussian) volume source with 4 levels of hopping-parameter variance reduction [75]. We use 24 stochastic sources per gauge configuration and evaluate the relevant propagators every 10-th trajectory.

## 4 Summary

In this letter we have presented results of simulations of lattice QCD with  $N_f = 2$  maximally twisted Wilson quarks at a fixed value of the lattice spacing  $a \lesssim 0.1$  fm. We reached a pseudo scalar meson mass of about 300 MeV. The numerical stability and smoothness of the simulations allowed us to obtain precise results for the pseudo scalar mass and decay constant which in turn led to determine the low energy constants of the effective chiral Lagrangian. In particular, we find for the pseudo scalar decay constant in the chiral limit  $F = 121.3(7)$  MeV, and  $\bar{l}_3 = 3.65(12)$  and  $\bar{l}_4 = 4.52(6)$  where only statistical errors are given.

We do see effects of isospin breaking which are largest in the mass splitting of the neutral and charged pions and turn out to be about 20%. This is significantly smaller and opposite in sign than the corresponding splitting obtained in the quenched approximation.

Tuning to maximal twist had to be performed on lattices of the same size as those used for the calculation of physical quantities. The reason for this is that we need to single out cleanly the one pion sector in order to impose the vanishing of the PCAC quark mass (Eq. (3)) without being affected by finite size effects or excited state contributions. Thus the tuning step itself is rather expensive. But it has to be done only once, as is the case for the determination of action improvement coefficients in other Wilson based approaches. Note, however, that with twisted mass fermions we do not have to compute further operator-specific improvement coefficients.

The encouraging results presented here will be extended and checked by future simulations that will cover one coarser and one finer lattice spacing, double the statistics at one of our present simulation points ( $\beta = 3.9, a\mu = 0.004$ ) and go to a larger,  $32^3 \cdot 64$ , volume at the latter simulation point. In this way, we will be able to obtain results in the continuum limit, cross-check our autocorrelation times, improve our error estimates and control the finite size effects in order to check  $\chi$ PT predictions. The preliminary results presented in Refs. [32, 33] indicate a very good scaling behaviour already suggesting that automatic  $\mathcal{O}(a)$  improvement is indeed working well.

## Acknowledgments

The computer time for this project was made available to us by the John von Neumann-Institute for Computing on the JUMP and Jubl systems in Jülich and apeNEXT system in Zeuthen, by UKQCD on the QCDOC machine at Edinburgh, by INFN on the apeNEXT systems in Rome, by BSC on MareNostrum in Barcelona ([www.bsc.es](http://www.bsc.es)) and by the Leibniz Computer centre in Munich on the Altix system. We thank these computer centres and their staff for all technical advice and help. On QCDOC we have made use of Chroma [76] and BAGEL [77] software and we thank members of UKQCD for assistance. For the analysis we used among others the R language for statistical computing [78]. We gratefully acknowledge discussions with D. Bećirević, B. Blossier, N. Christian, G. Münster, O. Pène and A. Vladikas.

This work has been supported in part by the DFG Sonderforschungsbereich/Transregio SFB/TR9-03 and the EU Integrated Infrastructure Initiative Hadron Physics (I3HP) under contract RII3-CT-2004-506078. We also thank the DEISA Consortium (co-funded by the EU, FP6 project 508830), for support within the DEISA Extreme Computing Initiative ([www.deisa.org](http://www.deisa.org)). G.C.R. and R.F. thank MIUR (Italy) for partial financial support under the contract PRIN04. V.G. and D.P. thank MEC (Spain) for partial financial support under

grant FPA2005-00711.

## References

- [1] K. G. Wilson, Phys. Rev. **D10**, 2445 (1974).
- [2] ALPHA, R. Frezzotti, P. A. Grassi, S. Sint and P. Weisz, JHEP **08**, 058 (2001), [hep-lat/0101001].
- [3] R. Frezzotti and G. C. Rossi, JHEP **08**, 007 (2004), [hep-lat/0306014].
- [4] M. Hasenbusch, Phys. Lett. **B519**, 177 (2001), [hep-lat/0107019].
- [5] TrinLat, M. J. Peardon and J. Sexton, Nucl. Phys. Proc. Suppl. **119**, 985 (2003), [hep-lat/0209037].
- [6] QCDSF, A. Ali Khan *et al.*, Phys. Lett. **B564**, 235 (2003), [hep-lat/0303026].
- [7] M. Lüscher, Comput. Phys. Commun. **165**, 199 (2005), [hep-lat/0409106].
- [8] C. Urbach, K. Jansen, A. Shindler and U. Wenger, Comput. Phys. Commun. **174**, 87 (2006), [hep-lat/0506011].
- [9] M. A. Clark and A. D. Kennedy, hep-lat/0608015.
- [10] L. Del Debbio, L. Giusti, M. Lüscher, R. Petronzio and N. Tantalo, JHEP **02**, 011 (2006), [hep-lat/0512021].
- [11] R. Frezzotti and G. C. Rossi, JHEP **10**, 070 (2004), [hep-lat/0407002].
- [12] R. Frezzotti, G. Martinelli, M. Papinutto and G. C. Rossi, JHEP **04**, 038 (2006), [hep-lat/0503034].
- [13] S. R. Sharpe and J. M. S. Wu, Phys. Rev. **D71**, 074501 (2005), [hep-lat/0411021].
- [14] S. R. Sharpe, Phys. Rev. **D72**, 074510 (2005), [hep-lat/0509009].
- [15] S. Aoki and O. Bär, Phys. Rev. **D70**, 116011 (2004), [hep-lat/0409006].
- [16]  $\chi_{\text{L}}^{\text{F}}$ , K. Jansen, A. Shindler, C. Urbach and I. Wetzorke, Phys. Lett. **B586**, 432 (2004), [hep-lat/0312013].
- [17]  $\chi_{\text{L}}^{\text{F}}$ , K. Jansen, M. Papinutto, A. Shindler, C. Urbach and I. Wetzorke, Phys. Lett. **B619**, 184 (2005), [hep-lat/0503031].
- [18]  $\chi_{\text{L}}^{\text{F}}$ , K. Jansen, M. Papinutto, A. Shindler, C. Urbach and I. Wetzorke, JHEP **09**, 071 (2005), [hep-lat/0507010].

- [19] A. M. Abdel-Rehim, R. Lewis and R. M. Woloshyn, Phys. Rev. **D71**, 094505 (2005), [hep-lat/0503007].
- [20] C. Pena, S. Sint and A. Vladikas, JHEP **09**, 069 (2004), [hep-lat/0405028].
- [21] ALPHA, M. Guagnelli, J. Heitger, C. Pena, S. Sint and A. Vladikas, JHEP **03**, 088 (2006), [hep-lat/0505002].
- [22] ALPHA, P. Dimopoulos *et al.*, Nucl. Phys. **B749**, 69 (2006), [hep-ph/0601002].
- [23] D. Becirevic *et al.*, Phys. Rev. **D74**, 034501 (2006), [hep-lat/0605006].
- [24] T. Chiarappa *et al.*, hep-lat/0606011.
- [25] E. M. Ilgenfritz *et al.*, hep-lat/0610112.
- [26] O. Bär, K. Jansen, S. Schaefer, L. Scorzato and A. Shindler, hep-lat/0609039.
- [27]  $\chi_{\text{F}}$ , K. Jansen *et al.*, Phys. Lett. **B624**, 334 (2005), [hep-lat/0507032].
- [28] F. Farchioni *et al.*, PoS **LAT2005**, 033 (2006), [hep-lat/0509036].
- [29] F. Farchioni *et al.*, PoS **LAT2005**, 072 (2006), [hep-lat/0509131].
- [30] L. Scorzato *et al.*, Nucl. Phys. Proc. Suppl. **153**, 283 (2006), [hep-lat/0511036].
- [31] A. Shindler, PoS **LAT2005**, 014 (2006), [hep-lat/0511002].
- [32] ETM, K. Jansen and C. Urbach, hep-lat/0610015.
- [33] ETM, A. Shindler, hep-ph/0611264.
- [34] ETM Collaboration, P. Boucaud *et al.*, in preparation (2007).
- [35] L. Del Debbio, L. Giusti, M. Lüscher, R. Petronzio and N. Tantalo, hep-lat/0610059.
- [36] L. Del Debbio, L. Giusti, M. Lüscher, R. Petronzio and N. Tantalo, hep-lat/0701009.
- [37] M. Gockeler *et al.*, PoS. **LAT2006**, 179 (2006), [hep-lat/0610066].
- [38] P. Weisz, Nucl. Phys. **B212**, 1 (1983).
- [39] F. Farchioni *et al.*, Nucl. Phys. Proc. Suppl. **140**, 240 (2005), [hep-lat/0409098].



- [40] F. Farchioni *et al.*, Eur. Phys. J. **C42**, 73 (2005), [hep-lat/0410031].
- [41] F. Farchioni *et al.*, Eur. Phys. J. **C39**, 421 (2005), [hep-lat/0406039].
- [42] F. Farchioni *et al.*, Eur. Phys. J. **C47**, 453 (2006), [hep-lat/0512017].
- [43] F. Farchioni *et al.*, Phys. Lett. **B624**, 324 (2005), [hep-lat/0506025].
- [44] S. R. Sharpe and J. M. S. Wu, Phys. Rev. **D70**, 094029 (2004), [hep-lat/0407025].
- [45] G. Münster, JHEP **09**, 035 (2004), [hep-lat/0407006].
- [46] G. Münster, C. Schmidt and E. E. Scholz, Nucl. Phys. Proc. Suppl. **140**, 320 (2005), [hep-lat/0409066].
- [47] L. Scorzato, Eur. Phys. J. **C37**, 445 (2004), [hep-lat/0407023].
- [48] S. Aoki, Phys. Lett. **B190**, 140 (1987).
- [49] A. Sternbeck, E.-M. Ilgenfritz, W. Kerler, M. Müller-Preußker and H. Stüben, Nucl. Phys. Proc. Suppl. **129**, 898 (2004), [hep-lat/0309059].
- [50] E.-M. Ilgenfritz, W. Kerler, M. Müller-Preußker, A. Sternbeck and H. Stüben, Phys. Rev. **D69**, 074511 (2004), [hep-lat/0309057].
- [51] T. Blum *et al.*, Phys. Rev. **D50**, 3377 (1994), [hep-lat/9404006].
- [52] JLQCD, S. Aoki *et al.*, Nucl. Phys. Proc. Suppl. **106**, 263 (2002), [hep-lat/0110088].
- [53] JLQCD, S. Aoki *et al.*, hep-lat/0409016.
- [54] K. Jansen, Nucl. Phys. Proc. Suppl. **129**, 3 (2004), [hep-lat/0311039].
- [55] M. Creutz, hep-lat/9608024.
- [56] S. R. Sharpe and J. Singleton, R., Phys. Rev. **D58**, 074501 (1998), [hep-lat/9804028].
- [57] S. Aoki and K. Higashijima, Prog. Theor. Phys. **76**, 521 (1986).
- [58] T. Izubuchi, J. Noaki and A. Ukawa, Phys. Rev. **D58**, 114507 (1998), [hep-lat/9805019].
- [59] K.-i. Nagai and K. Jansen, Phys. Lett. **B633**, 325 (2006), [hep-lat/0510076].
- [60] QCD-TARO, P. de Forcrand *et al.*, Nucl. Phys. Proc. Suppl. **53**, 938 (1997), [hep-lat/9608094].

- [61] T. DeGrand, A. Hasenfratz and T. G. Kovacs, Phys. Rev. **D67**, 054501 (2003), [hep-lat/0211006].
- [62] S. Necco, Nucl. Phys. **B683**, 137 (2004), [hep-lat/0309017].
- [63] S. Takeda *et al.*, Phys. Rev. **D70**, 074510 (2004), [hep-lat/0408010].
- [64] QCDSF, R. Horsley, H. Perlt, P. E. L. Rakow, G. Schierholz and A. Schiller, Nucl. Phys. **B693**, 3 (2004), [hep-lat/0404007].
- [65] M. Hasenbusch and K. Jansen, Nucl. Phys. **B659**, 299 (2003), [hep-lat/0211042].
- [66] UKQCD, M. Foster and C. Michael, Phys. Rev. **D59**, 074503 (1999), [hep-lat/9810021].
- [67] UKQCD, C. McNeile and C. Michael, Phys. Rev. **D73**, 074506 (2006), [hep-lat/0603007].
- [68] UKQCD, P. Lacock, A. McKerrell, C. Michael, I. M. Stopher and P. W. Stephenson, Phys. Rev. **D51**, 6403 (1995), [hep-lat/9412079].
- [69] ALPHA, U. Wolff, Comput. Phys. Commun. **156**, 143 (2004), [hep-lat/0306017].
- [70] R. Sommer, Nucl. Phys. **B411**, 839 (1994), [hep-lat/9310022].
- [71] J. Gasser and H. Leutwyler, Phys. Lett. **B184**, 83 (1987).
- [72] G. Colangelo, S. Dürr and C. Haefeli, Nucl. Phys. **B721**, 136 (2005), [hep-lat/0503014].
- [73] H. Leutwyler, hep-ph/0612112.
- [74] A. Walker-Loud and J. M. S. Wu, Phys. Rev. **D72**, 014506 (2005), [hep-lat/0504001].
- [75] UKQCD, C. McNeile and C. Michael, Phys. Rev. **D63**, 114503 (2001), [hep-lat/0010019].
- [76] R. G. Edwards and B. Joo, Nucl. Phys. Proc. Suppl. **140**, 832 (2005), [hep-lat/0409003].
- [77] P. Boyle, <http://www.ph.ed.ac.uk/~paboyle/bagel/Bagel.html>.
- [78] R Development Core Team, *R: A language and environment for statistical computing*, R Foundation for Statistical Computing, Vienna, Austria, 2005, ISBN 3-900051-07-0.